

## Peridotite-Gabbro-Basalt Complex from the Equatorial Mid-Atlantic Ridge

E. Bonatti, J. Honnorez and G. Ferrara

*Phil. Trans. R. Soc. Lond. A* 1971 **268**, 385-402

doi: 10.1098/rsta.1971.0002

### Email alerting service

Receive free email alerts when new articles cite this article - sign up in the box at the top right-hand corner of the article or click [here](#)

## I. ULTRAMAFIC ROCKS

## Peridotite–gabbro–basalt complex from the equatorial Mid-Atlantic Ridge

BY E. BONATTI,†, J. HONNOREZ† AND G. FERRARA‡

† *Institute of Marine Sciences, University of Miami, Florida, U.S.A.*‡ *Department of Earth Sciences, University of Pisa, Italy*

[Plate 1]

Rocks were dredged where the Mid-Atlantic Ridge is intersected by the Chain, Romanche, St Paul and Vema Fracture Zones, and from unfractured portions of the Ridge between 6 and 8° N. Peridotites are common at the fracture zones, but were found also in unfractured sections of the Ridge; harzburgites prevail, but lherzolites, dunites and plagioclase peridotites are also present. A variety of gabbros was recovered, generally above the peridotites, including norites, troctolites, quartz gabbros and theralites. The chemistry of these gabbros indicates a marked crystal–liquid fractionation, following both a ‘tholeiitic’ and an ‘alkali’ trend. The basalts show also both trends, but less markedly. Metamorphic rocks ranging from ‘greenschist’ to ‘amphibolite’ facies are found throughout the sections. Strontium isotopic data suggest that the peridotites (excluding St Peter–Paul rocks) are not related genetically to the associated gabbro–basalt, in a situation similar to that of alpine complexes on the continents. The peridotites are probably residual and were depleted of lithophile elements at some early stage of their history, before the opening of the Atlantic rift. It is postulated that in the upper mantle below the equatorial Atlantic a zone exists of residual, alpine-type peridotite, while the lower crust consists of a mixture of ultramafics and intrusive gabbros. The data indicate strong similarities between the Mid-Atlantic Ridge and alpine complexes from various parts of the world.

## INTRODUCTION

Various hypothesis have been formulated on the nature of the oceanic crust and upper mantle. Hess (1962) suggested that the lower oceanic crust (seismic layer 3, with velocities close to  $6.7 \text{ km s}^{-1}$ ) is composed of serpentinized peridotite, overlain by a basaltic layer (seismic layer 2, velocities of about  $5.0 \text{ km s}^{-1}$ ) and by a thin cover of unconsolidated sediment. Cann (1968) and Christiansen (1970) proposed instead a layer 3 of basaltic composition, made of amphibolite. Several models have been proposed for the composition of the oceanic upper mantle, most authors agreeing on some type of peridotitic material as its most probable component. A test of these hypothesis can be provided by direct sampling of the crust beneath the ocean, which is possible only where sediment cover is absent and where thick crustal sections are exposed. This situation is verified where active oceanic ridges are intersected by tectonic fracture zones. The equatorial Mid-Atlantic Ridge (M.A.R.) offers the possibility of achieving such sampling of the oceanic crust, since its axis is cut and displaced by major, deep tectonic fractures, such as the Vema Fracture Zone at 10° N, the St Paul F.Z. at 0°, the Romanche F.Z. at 2° S, the Chain F.Z. at 3° S. A series of dredgings were made in this region both at the intersection of the ridge with the fracture zones, and also in sections across unfractured portions of the Ridge. This paper presents a preliminary evaluation of the material recovered, which we hope will contribute to clarify our concepts on the constitution of the oceanic upper mantle and crust.

Figure 1 shows schematically the location of the dredge hauls and the rock types recovered at the various stations. Table 1 gives a brief petrological description of the various samples. Additional dredgings were made recently in the Vema F.Z., as shown in figure 2.

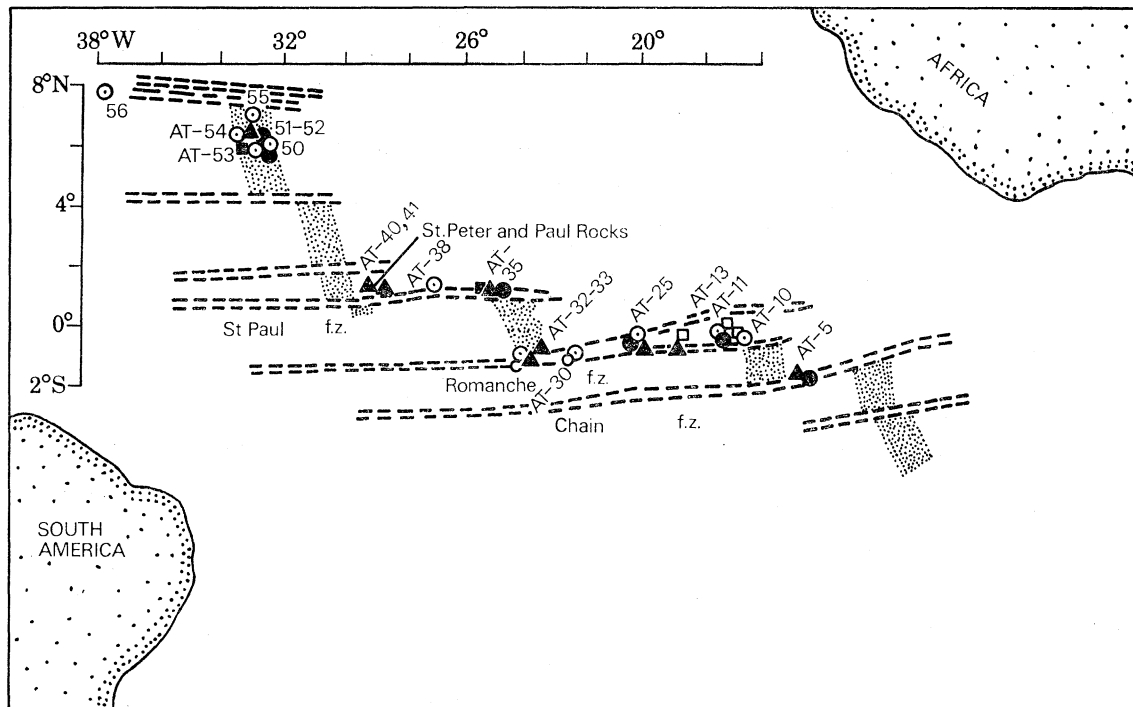


FIGURE 1. Approximate location of rocks dredged at the equatorial M.A.R. during cruises P6707 and P6903 of the R.V. *Pillsbury*, Institute of Marine Sciences, University of Miami. Dotted areas, crest of Mid-Atlantic Ridge; ---, fracture zones; ■, amphibolitic facies; □, greenschist facies; ▲, peridotites; ○, alkali basalts and dolerites; ⊙, other basalts; ●, gabbros, norite, qz-diorites and nepheline gabbro.

## PERIDOTITES FROM THE MID-ATLANTIC RIDGE

### *Field relationships*

Ultramafic rocks were dredged by us within three different geological settings:

(a) Where the Mid-Atlantic Ridge is interrupted by an east-west valley associated with a fracture zone, portions of deep crust below the ridge are exposed. Peridotites were dredged at such sites, below a gabbro-basalt layer. An example of such situation is just north of the Vema Fracture Zone (figure 2).

(b) Transverse east-west ridges associated with and parallel to the transform faults which displace the axis of M.A.R. are made essentially of ultramafic rocks. In a section across a transverse ridge in the Romanche F.Z. ultramafics have been found to outcrop up to the crest of the ridge (figure 3). A transverse ridge associated with the Vema F.Z. is primarily made of ultramafics (Van Andel, Corliss & Bowen, 1967; E. Bonatti & J. Honnorez, in preparation). Van Andel (1970) reports that transverse ridges in the Ascension F.Z. are peridotitic.

(c) At least in one case a serpentized peridotite (sample P6903-28 in table 1) was dredged from the wall of the central rift valley, in a portion of the Ridge which is not intersected by east-west fracture zones (figure 4). The recovery of peridotite from this locality is remarkable

ULTRAMAFIC ROCKS

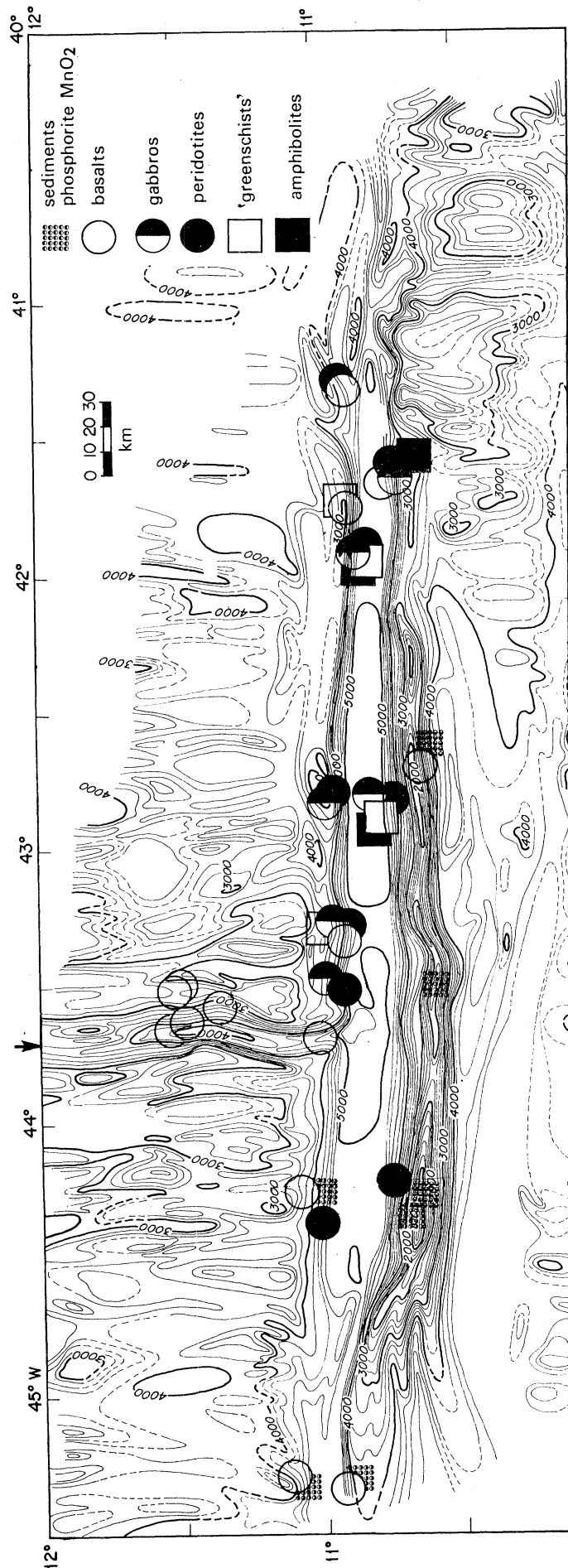


FIGURE 2. Types of rocks dredged during cruise P7003 at the Vema F.Z. Bathymetry is by Van Andel *et al.* (1967) from surveys of Scripps and Woods Hole vessels. Where the M.A.R. is interrupted by the east-west valley a steep cliff is present (north wall of the east-west valley). In several sections across this cliff peridotites, amphibolites, gabbros and basalts were dredged. Arrows indicate the axis of the M.A.R. north and south of the fracture.

TABLE 1. SIMPLIFIED PETROLOGIC DESCRIPTION OF ROCKS DREDGED DURING  
CRUISES P6707 AND P6903 (SEE FIGURE 1)

Only the major mineral components are mentioned. The term 'basalt' indicates here all basaltic rocks excluding those showing clear evidence of alkali affinities, which are indicated as 'alkali basalts'. The term 'greenschist' indicates rocks belonging to the greenschist facies.

station number, location and depth	petrographic description
P6707B-5; 01° 07' S, 14° 52' W (northern wall of Chain Fracture); 5370-5170 m	<i>harzburgites</i> (serpentinized): enstatite with exsolution lamellae of clinopyroxene, forsterite, picotite and serpentine; mylonitic <i>norite</i> (uralitized): hypersthene and calcic plagioclase, with secondary chlorite, antophyllite, hornblende, grunerite, epidote and zoisite; cataclastic <i>olivine gabbro</i> (uralitized): enstatite and calcic plagioclase with hornblende and olivine; secondary antophyllite, talc and chlorite
P6707B-8; 00° 24' N, 17° 05' W (northern wall of Romanche Fracture); 900-1000 m	MnO <sub>2</sub> encrusted limestones and phosphorites
P6707B-9; 00° 24' N, 17° 05' W (northern wall of Romanche Fracture); 1100-1200 m	MnO <sub>2</sub> encrusted limestones and phosphorites
P6707B-10; 00° 24' N, 17° 05' W (northern wall of Romanche Fracture); 2560-2450 m	<i>basalts</i> : calcic plagioclase, pigeonitic clinopyroxene, serpentine and talc pseudomorphs after olivine <i>metabasaltic breccias</i> : elements of microlitic basalt cemented by zoisite and epidote
P6707B-11; 00° 18' N, 17° 14' W (northern wall of Romanche Fracture); 5305-5100 m	<i>gabbros</i> (uralitized): diopsidic clinopyroxene and calcic plagioclase with some secondary actinolite, hornblende and chlorite; locally rich in magnetite and ilmenite; cataclastic <i>quartz diorite</i> (uralitized) as vein in gabbro: calcic plagioclase, quartz and biotite with secondary actinolite, hornblende and chlorite; cataclastic <i>low-grade metabasalts</i> : calcic plagioclase with albite rims, pigeonitic clinopyroxene with actinolite and chlorite rims, veins of prehnite, analcite, talc and antigorite ' <i>greenschists</i> ': bands rich in albite and chlorite alternating with chlorite-actinolitic bands; veins of epidote, chlorite, albite and quartz <i>metabasaltic breccia</i> : elements of metabasalts cemented by epidote, zoisite, prehnite, analcite, and forsterite
P6707B-13; 00° 18.5' S, 18° 26' W (southern wall of Romanche Fracture); 5940-5700 m	<i>dunites</i> (serpentinized): forsterite, picotite and serpentine; cataclastic <i>harzburgites</i> (serpentinized): enstatite with clinopyroxene exsolution lamellae, forsterite and serpentine; cataclastic <i>plagioclase harzburgite</i> (serpentinized): enstatite with clinopyroxene exsolution lamellae, forsterite, accessory calcic plagioclase and serpentine; cataclastic <i>lherzolite</i> (serpentinized): diopside, enstatite, forsterite and serpentine; cataclastic <i>carbonate breccia</i> : fragments of serpentine in a calcite-aragonite cement
P6707B-25; 00° 22' S, 20° 09' W (northern wall of Romanche Fracture); 5200-5100 m	<i>harzburgites</i> (serpentinized): enstatite with clinopyroxene exsolution lamellae, forsterite, picotite and serpentine; cataclastic <i>gabbros</i> (uralitized): diopsidic clinopyroxene and calcic plagioclase, hypersthene, with accessory chloramphibole; cataclastic

## ULTRAMAFIC ROCKS

389

TABLE 1 (cont.)

station number, location and depth	petrographic description
	<i>olivine gabbros</i> (uralitized): talc, serpentine, amphibole pseudo-morphs after olivine, with calcic plagioclase, hornblende, accessory chlorite and zoisite; cataclastic
	<i>nepheline gabbro</i> : titanaugite with calcic plagioclase, nepheline and natrolite, minor aegyrine, barkevikite and magnetite; secondary chlorite
	<i>alkali basalt</i> : calcic plagioclase, titanaugite, serpentinized olivine
	<i>palagonite breccia</i> : glass, fragments cemented by carbonates
P 6707B-30; 01° 22' S, 22° 46' W (northern wall of Romanche Fracture); 4850–3500 m	<i>basalt</i> : calcic plagioclase, pigeonitic pyroxene, serpentinized olivine <i>alkali basalt</i> : calcic plagioclase, titanaugite, serpentinized olivine
P 6707B-32; 00° 56.3' S, 24° 04.7' W (northern wall of Romanche Fracture); 2750–1380 m	<i>harzburgites</i> (serpentinized): forsterite, enstatite with clinopyroxene exsolution lamellae, picotite, and serpentine; cataclastic to mylonitic <i>plagioclase harzburgite</i> (serpentinized): forsterite, enstatite with clinopyroxene exsolution lamellae, picotite, accessory calcic plagioclase, and serpentine; cataclastic
P 6707B-33; 01° 08' S; 24° 05' W (northern wall of Romanche Fracture); 5200–4800 m	<i>harzburgites</i> (serpentinized): forsterite, enstatite with clinopyroxene exsolution lamellae, picotite and serpentine; cataclastic <i>serpentine-chlorite breccia</i> : serpentine and chlorite elements with chloramphibole, epidote, diopside, hypersthene and hornblende grains in a matrix of prehnite <i>alkali basalt</i> : calcic plagioclase, titanaugite, serpentine pseudo-morphs after olivine
P 6707B-35; 00° 52' N, 25° 05.5' W (St Paul Fracture); 4000–3700 m	<i>serpentinites</i> : rare picotite in a matrix of serpentine; cataclastic <i>gabbros</i> (uralitized): diopside, calcic plagioclase and orthopyroxene <i>quartz gabbro</i> (uralitized): diopside, calcic plagioclase, quartz, biotite; slightly cataclastic <i>amphibolitized basalts</i> : calcic plagioclase and clinopyroxene partly or totally replaced by actinolite and hornblende
P 6707B-40; 00° 56' N, 29° 34' W (3 km NW of St Paul Rocks); 1100–700 m	<i>harzburgites</i> (serpentinized): forsterite, enstatite with exsolution lamellae of clinopyroxene, picotite and serpentine; rare hornblende phenoclasts; (mylonitic)
P 6707B-41; 00° 55' N, 29° 31' W (6½ km SE of St Paul Rocks); 3000–2000 m	as above
P 6903-26; 05° 55' N, 33° 14.9' W (west wall of central rift valley); 4660–4260 m	<i>basalt</i> : skeletal microphenocrysts of calcic plagioclase, augite and forsterite in glassy groundmass ' <i>greenschist</i> ': penninite, quartz, albite and epidote <i>granular amphibolites</i> : calcic plagioclase and tremolite or antophyllite grading into hornblende; cataclastic to mylonitic <i>banded amphibolites</i> : the same as above but microcrystalline and with parallel bands rich in plagioclase alternating with hornblende bands (not cataclastic) <i>amphibolitized basalts, basaltic breccias, gabbros, peridotites</i> with transitional stages between greenschist facies and amphibolite facies
P 6903-27; 06° 00.5' N, 33° 16.5' W (west wall of central rift valley); 3300–3660 m	<i>granular amphibolite</i> : calcic plagioclase and hornblende <i>basalt</i> : fresh glass with rare olivine microphenocrysts

TABLE 1 (*cont.*)

station number, location and depth	petrographic description
P6903-28; 06° 00.5' N, 33° 16.5' W (west wall of central rift valley); 3260-3200 m	<i>serpentinite</i> : rare picotite in a matrix of serpentine; mylonitic <i>amphibolitized dunite</i> : large crystals of forsterite surrounded by four successive rims of (1) serpentine+magnetite, (2) talc+magne- netite, (3) antophyllite, (4) cummingtonite <i>basalts</i> : calcic plagioclase, augite and forsterite microphenocrysts either in a glassy matrix or largely crystallized (diabase)
P6903-29; 05° 53' N, 33° 14.5' W (west wall of central rift valley); 3200-3100 m	<i>chloritoschist</i> : quartz and opaques in a matrix of penninite grading into antophyllite <i>amphiboloschists</i> : albite and quartz associated with hornblende and relicts of serpentized orthopyroxene <i>talcschist</i> : penninite with serpentine and actinolite-tremolite in a matrix of talc <i>quartz</i> : fragment of a large, polycrystalline vein of quartz
P6903-30; 05° 51.4' N, 33° 26.5' W (west wall of central rift valley); 3150-2930 m	<i>basalt</i> : skeletal microphenocrysts of calcic plagioclase, clino- pyroxene and forsterite in glassy matrix
P6903-34; 07° 09' N, 33° 58' W (west wall of central rift valley); 4450-4070 m	<i>basalt</i> : as above
P6903-40; 07° 49' N, 38° 02.5' W (west wall of central rift valley); 5530-5320 m	<i>basalt</i> : phenocrysts of bytownite and forsterite in glassy groundmass

because it suggests that peridotites are generally present in the crust below the central zone of the M.A.R., and are not limited to fracture zones. Remarkable is also the fact that amphibolites were dredged below peridotites in this area (figure 4); the significance of this observation will be discussed further on.

#### *Textures*

Most of the ultramafic samples display clear signs of having been emplaced tectonically. Tectonic breccias, consisting of peridotitic fragments in a calcite-aragonite cement, have been found at some stations (figure 5); there is evidence that the carbonate cement was precipitated from hydrothermal solutions rising along tectonic fractures (Bonatti, Emiliani & Honnorez 1970). Samples with slickensided surfaces (figure 5) and with strain fabrics (figure 5) are common. All the peridotites display in thin section cataclastic or mylonitic textures.

#### *Mineralogy*

Some of the ultramafics are totally serpentized, but in most of the samples serpentization has been partial and primary phases are recognizable. The majority of the samples consist of the assemblage olivine (85 to 95 % forsterite), enstatite with clinopyroxene exsolution lamellae, and chromium-spinel; thus they could be classified as harzburgites. In some samples the clinopyroxene is abundant (Iherzolites), while in others both pyroxenes are absent (dunites). At two stations plagioclase-peridotites were recovered. Electron probe analyses of the primary phases are in progress.

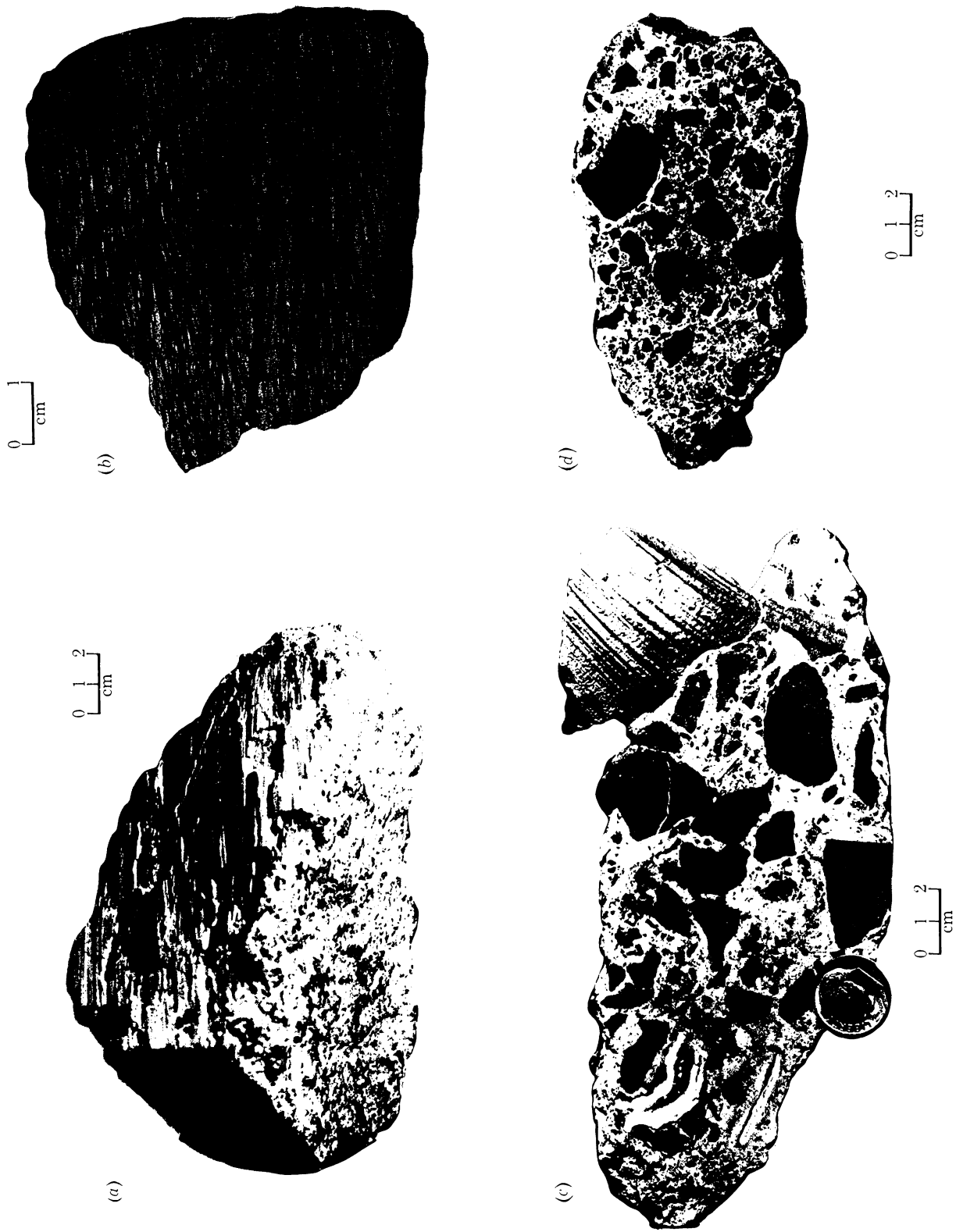


FIGURE 5. Photographs of rock specimens from the equatorial M.A.R. A, slickensided surface on peridotite from Romanche F.Z.; B, strain fabrics in serpentinite from Romanche F.Z.; C, peridotite breccia in calcite-aragonite matrix from Romanche F.Z.; D, same as C, from the Verna F.Z.



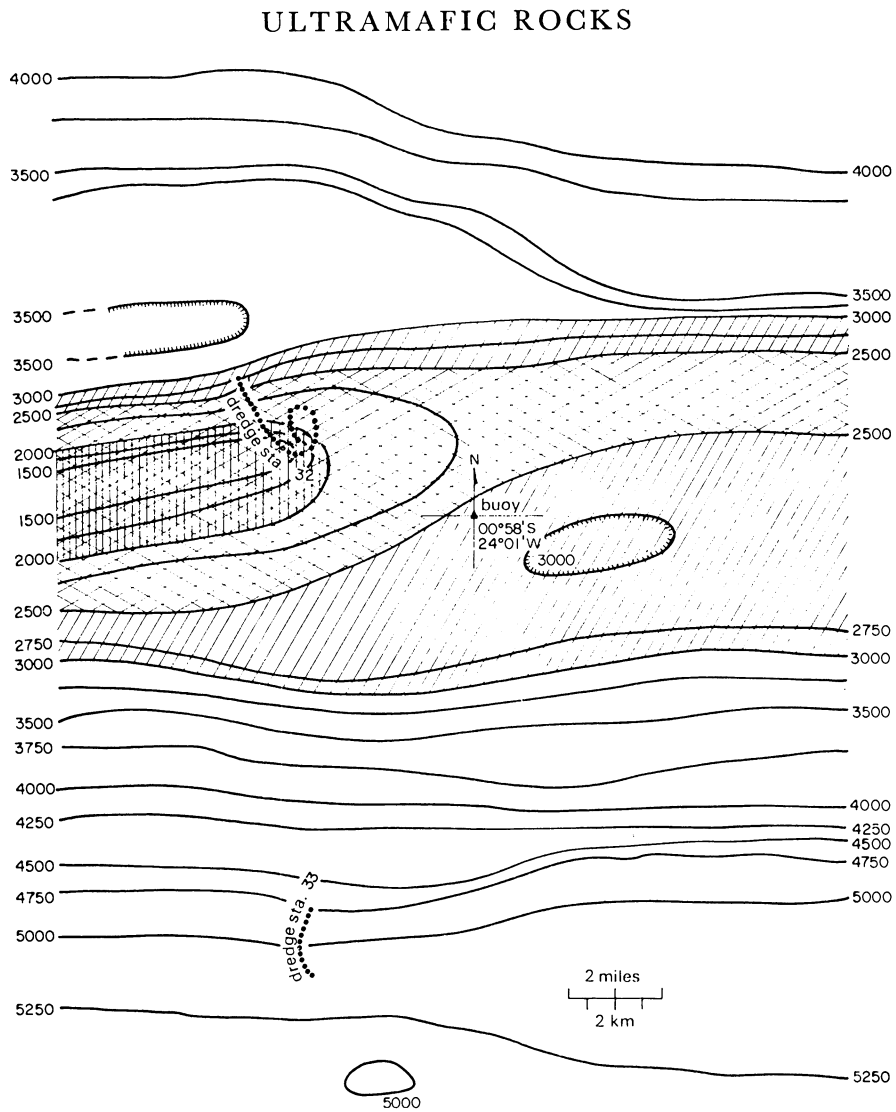


FIGURE 3. Topography of a portion of an east-west, transverse ridge associated with the Romanche Fracture Zone. Ultramafic rocks were recovered both from the lower slope and from the summit of the ridge.

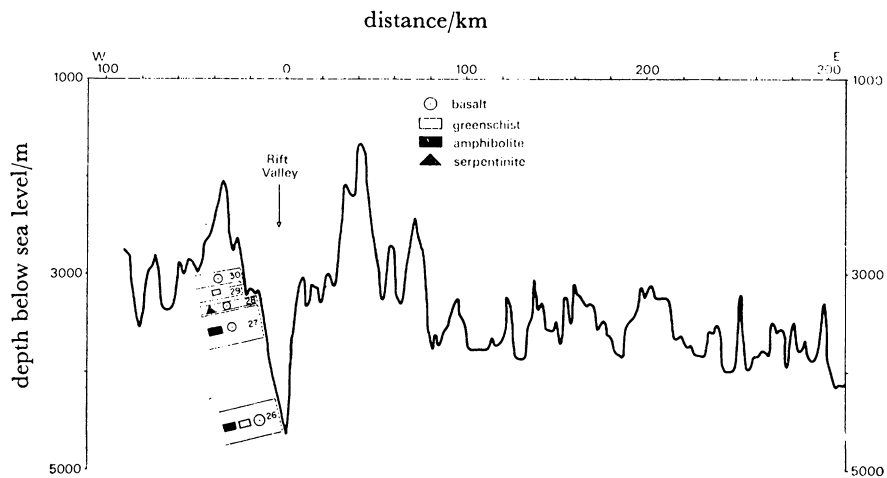


FIGURE 4. East-west topographic section of the axis of the M.A.R. at about 6° N. Dredgings were made on the western wall of the central rift valley. Rock types are indicated in the figure.

*Bulk chemistry*

If we assume that the peridotites from the equatorial M.A.R. represent material intruded into the crust from the upper mantle, and considering that these peridotites are closely associated with gabbros and basalts, the following questions arise: can the chemistry of the M.A.R. ultramafics clarify our concept on the nature of the oceanic upper mantle, and what is the relation between the ultramafics and the gabbros and basalts in the M.A.R. complex?

TABLE 2. CHEMICAL ANALYSES OF FIVE PERIDOTITES FROM THE EQUATORIAL M.A.R.

	Analyst: R. Mazzuoli.				
	P 6707-5	P 6707-13	P 6707-25	P 6707-33	P 6903-28
SiO <sub>2</sub>	38.55	42.36	40.45	37.62	37.28
Al <sub>2</sub> O <sub>3</sub>	2.04	3.36	2.73	1.72	2.07
Fe <sub>2</sub> O <sub>3</sub>	7.23	5.51	5.14	5.45	8.86
FeO	1.76	3.07	2.32	1.44	1.62
CaO	0.37	2.24	1.12	0.50	0.21
MgO	35.88	36.48	34.47	37.80	36.57
MnO	0.41	0.10	0.11	0.05	0.11
Na <sub>2</sub> O	0.42	0.62	0.17	0.16	0.28
K <sub>2</sub> O	0.05	0.03	0.04	0.02	0.02
Ti <sub>2</sub> O	0.04	0.10	0.41	0.03	0.24
P <sub>2</sub> O <sub>5</sub>	trace	trace	0.11	0.04	0.05
Cr <sub>2</sub> O <sub>3</sub>	0.46	0.39	0.29	0.39	0.52
NiO	0.21	0.26	0.24	0.26	0.24
H <sub>2</sub> O <sup>-</sup>	1.01	0.50	1.01	0.96	0.48
H <sub>2</sub> O <sup>+</sup>	11.55	4.62	11.46	13.02	11.92
total	99.98	99.68	100.07	99.46	100.47

TABLE 3. CHEMICAL ANALYSES OF PERIDOTITES FROM TABLE 2 RECALCULATED WATER-FREE AND COMPARED WITH SAMPLE 18-900 (MELSON *ET AL.* 1967) FROM THE ST PETER-PAUL MASSIF AND WITH TWO THEORETICAL PYROLITE COMPOSITIONS ACCORDING TO GREEN & RINGWOOD (1963)

						St Paul	Pyr 1	Pyr 2
	P 6707-5	P 6707-13	P 6707-25	P 6707-33	P 6903-28	18-900		
SiO <sub>2</sub>	44.09	44.79	46.17	44.01	42.32	44.78	42.97	43.33
Al <sub>2</sub> O <sub>3</sub>	2.33	3.55	3.11	2.01	2.35	4.68	3.32	4.01
Fe <sub>2</sub> O <sub>3</sub>	8.27	5.83	5.86	6.37	10.06	3.03	1.58	1.67
FeO	2.01	3.24	2.64	1.68	1.83	4.72	6.55	6.70
CaO	0.42	2.36	1.27	0.58	0.23	4.15	2.12	2.67
MgO	41.04	38.57	39.34	44.22	41.52	36.71	41.66	39.57
MnO	0.46	0.10	0.12	0.05	0.12	0.13	0.13	0.13
Na <sub>2</sub> O	0.47	0.65	0.19	0.18	0.30	0.45	0.49	0.61
K <sub>2</sub> O	0.05	0.03	0.04	0.02	0.02	0.11	0.18	0.22
TiO <sub>2</sub>	0.04	0.10	0.46	0.03	0.26	0.31	0.47	0.58
P <sub>2</sub> O <sub>5</sub>	—	—	0.12	0.04	0.05	0.05	0.06	0.08
Cr <sub>2</sub> O <sub>3</sub>	0.51	0.41	0.33	0.45	0.59	0.53	0.45	0.42

The results of chemical analyses of five ultramafic samples from the equatorial M.A.R. are shown in table 2. Three of the analyses had been presented previously (Bonatti 1968). In order to establish if the M.A.R. ultramafics are a possible parent material for oceanic basalts, the analyses of table 2 have been recalculated on a water-free basis and are compared in table 3 with two theoretical pyrolites (Green & Ringwood 1963) taken as approximating mantle material undepleted of basaltic components. In figure 6 a modified alkali-iron-magnesium diagram is presented, where the two Green-Ringwood pyrolites are compared with various

M.A.R. ultramafics, including those analysed by Miyashiro, Shido & Ewing (1969) and some from the St Peter–Paul massif analysed by Melson, Jarosewich, Bowen & Thompson (1967*a*). The diagram indicates that most of the M.A.R. peridotites are depleted in alkalis relative to the theoretical pyrolites, possible exceptions being a sample from the St Peter–Paul massif and a plagioclase peridotite (P6707–13) from the Romanche F.Z. Examination of table 3 shows that rock P6707–13 is strongly depleted in potassium relative to pyrolite. The only peridotite which could possibly be a parent material for oceanic basalt is sample 18–900 from the St Peter–Paul massif, as already pointed out by Melson, Jarosewich, Cifelli & Thompson (1967*b*). We conclude that with the exception of the aforementioned sample, the M.A.R. ultramafics considered here are probably residual.

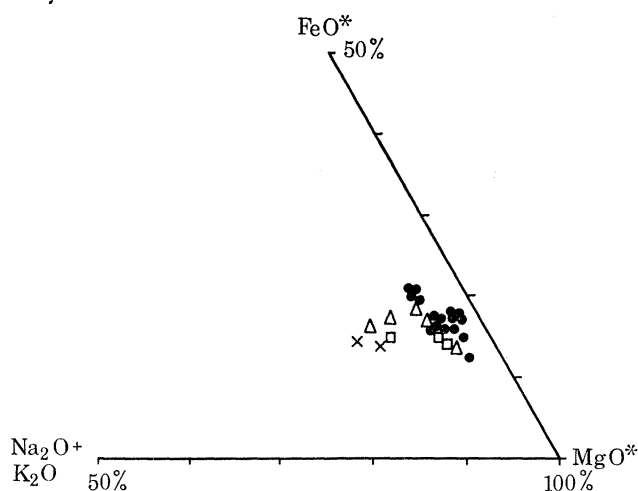


FIGURE 6. Portion of a modified alkali–iron–magnesium (A.F.M.) diagram for Atlantic ultramafic rocks and theoretical pyrolites. FeO\* indicates total iron as FeO. FeO\* and MgO\* have been multiplied by  $10^{-1}$ .  $\Delta$ , present work;  $\bullet$ , Miyashiro *et al.* (1969, 1970);  $\square$ , St Peter–Paul (Melson *et al.* 1967);  $\times$ , pyrolite.

#### *Strontium-isotopic chemistry*

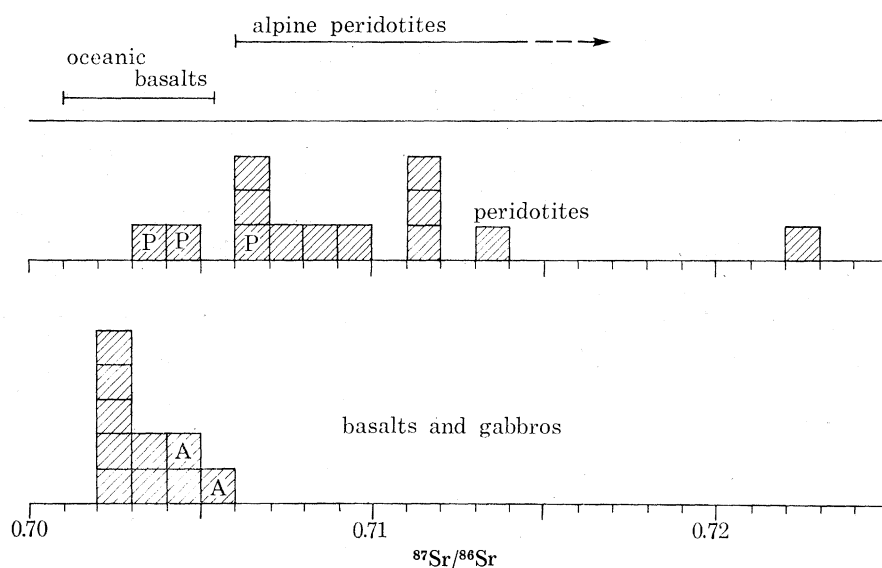
The significance of Rb/Sr and  $^{87}\text{Sr}/^{86}\text{Sr}$  data in determining genetical relations in igneous rock assemblages has been illustrated by various authors (see review by Hurley 1967). Rubidium, strontium and  $^{87}\text{Sr}/^{86}\text{Sr}$  were measured in peridotites, gabbros and basalts from the equatorial M.A.R. by mass spectrometry. The details of the methods and the error of the measurements are described in Bonatti, Ferrara & Honnorez (1970). The results are in table 4; the isotopic ratios are shown as histograms in figure 7.

The ratios  $^{87}\text{Sr}/^{86}\text{Sr}$  obtained in the M.A.R. samples are characterized by the fact that, while the basalts and gabbros have low ratios, in the range of values previously obtained for oceanic basalts (Hurley 1967), the ultramafic rocks (with the exception of samples from St Peter–Paul Islets and their vicinity) have ratios higher than 0.706 and reaching up to 0.723, that is, outside the basalt–gabbro range.

First, the possibility has to be considered that the high  $^{87}\text{Sr}/^{86}\text{Sr}$  ratios obtained for the peridotites are due to sea-water contamination, in view also of the low concentrations of strontium in the samples (table 4). Contamination, however, can be neglected for three reasons: (a) of a total of ten  $^{87}\text{Sr}/^{86}\text{Sr}$  values obtained (excluding again the values for St Peter–Paul), five are definitely higher than 0.709, the accepted value for sea water; thus, if contamination occurred, the original  $^{87}\text{Sr}/^{86}\text{Sr}$  values of these five samples had to be higher than the measured

TABLE 4. K, Rb, Sr, K/Rb, Rb/Sr AND  $^{87}\text{Sr}/^{86}\text{Sr}$  IN SOME OF THE BASALTS, GABBROS, AMPHIBOLITES AND PERIDOTITES FROM THE EQUATORIAL M.A.R.

rock type	sample	K %	Rb parts/ $10^6$	Sr parts/ $10^6$	K/Rb	Rb/Sr	$^{87}\text{Sr}/^{86}\text{Sr}$
peridotites	P6707-5a	0.025	0.55	11.45	455	0.048	0.7069
	P6707-13a	0.025	0.50	16.9	500	0.030	0.7063
	P6707-13f	0.042	0.49	9.6	857	0.051	0.7227
	P6707-32b	0.024	0.22	64.7	1090	0.003	0.7096
	P6707-33a	0.011	<0.1	6.3	>1100	<0.016	0.7114
	P6707-33c	0.021	0.77	7.6	273	0.101	0.7076
	P6707-35	0.041	2.28	18.5	180	0.123	0.7111
	P6707-35b	0.017	0.48	7.5	354	0.064	0.7089
	P6903-28a	0.017	0.10	4.1	1700	0.024	0.7138
	P6903-26c	0.025	—	6.4	—	—	0.7113
St Paul Rocks	P6707-40	0.100	4.2	0.73	238	5.75	0.7034
	P6707-41	0.042	1.7	8.2	247	0.207	0.7067
	SP. SE	0.050	1.06	51.4	472	0.021	0.7042
	Hart (1965)	—	0.6	27	—	—	0.704
basalts and gabbros	P6707-11a	0.085	0.50	103	1700	0.005	0.7022
	P6707-5M	0.100	6.4	122	156	0.052	0.7035
	P6707-52B	0.149	1.7	125	876	0.014	0.7020
	P6707-25D	0.39	2	217	195	0.009	0.7041
	P6903-40	0.127	0.74	158	1716	0.005	0.7026
	P6707-33N	0.34	10.8	214	315	0.050	0.7028
amphibolites	P6903-26J	0.091	0.67	128	1358	0.005	0.7042
	P6903-26c	0.058	0.19	147	3053	0.001	0.7052
nepheline gabbros	P6707-25f(a)	0.80	62	281	129	0.221	0.7038
	P6707-25f(b)	0.80	54	276	125	0.196	0.7026

FIGURE 7. Histogram showing the  $^{87}\text{Sr}/^{86}\text{Sr}$  values for peridotites, gabbros, amphibolites and basalts from the equatorial M.A.R. P indicates samples from the St Peter-Paul massif. A indicates samples of amphibolite. The range of  $^{87}\text{Sr}/^{86}\text{Sr}$  values reported in the literature for oceanic basalts and alpine-type peridotites are shown in the upper portion of the figure.

values; (b) if contamination had occurred, it could be expected that the samples with lower Sr concentrations would have been affected the most, that is, would have  $^{87}\text{Sr}/^{86}\text{Sr}$  values closest to that of sea water: table 4 shows that this is not the case; (c) of the three samples from St Peter–Paul Islets and their vicinity, two were dredged from 700 to 3000 m below sea level; the third one, from the southeast islet, probably also spent a considerable time below sea level during the extrusion of the massif; their  $^{87}\text{Sr}/^{86}\text{Sr}$  ratio, however, is low and shows no indication of sea-water contamination, even though the samples are strongly serpentinized; the  $^{87}\text{Sr}/^{86}\text{Sr}$  values for two of the samples are close to those obtained by Hart (1965) in rocks from the islets. On the basis of these arguments we are confident that the high  $^{87}\text{Sr}/^{86}\text{Sr}$  ratios of the M.A.R. peridotites are real and are not due to sea-water contamination.

Stueber & Murthy (1966) measured Rb, Sr and  $^{87}\text{Sr}/^{86}\text{Sr}$  in a large number of ultramafic rocks from various parts of the world and showed that alpine peridotites, contrary to the case of peridotitic inclusions in basalts and of peridotites from stratiform sheet complexes, have  $^{87}\text{Sr}/^{86}\text{Sr}$  values higher than the range of modern basalts. The values obtained by us in the M.A.R. peridotites are in the range found by Stueber & Murthy in alpine-type peridotites. These authors, on the basis of the measured Rb/Sr ratios, calculated growth lines for the  $^{87}\text{Sr}/^{86}\text{Sr}$  in alpine peridotites and found that such lines do not pass through a  $^{87}\text{Sr}/^{86}\text{Sr}$  value as low as that assumed for the primordial Earth (0.698) even when projected back to  $4.5 \times 10^9$  years ago. They concluded that the strontium in alpine-type ultramafics must have been part of a system or systems with higher Rb/Sr ratios than the present one at some earlier stage of their histories. That is, alpine-type peridotites are probably residual in nature, having been depleted of lithophile elements. The Rb/Sr ratios measured in the peridotites from the M.A.R. are low and fall in the range of ratios found by Stueber & Murthy for alpine-type ultramafics. Thus, the above considerations for alpine-type peridotites are valid also for peridotites from the M.A.R.

These data confirm that the M.A.R. peridotites studied by us are residual; in addition, they suggest that these peridotites are not related genetically to the gabbro–basalt complex they are associated with. Specifically, it appears that the peridotites are neither the parent material for the modern basalts of the M.A.R. nor the residual product after their extraction. In addition, it is unlikely that the M.A.R. peridotites are gravitative cumulates from large igneous bodies of basic average composition, of which the overlying gabbros and basalts would constitute the lighter components. This does not exclude the occurrence of gravitative layering within the gabbro–basalt layer, as discussed in the next section.

These considerations do not apply to the mylonitized peridotites from the St Peter–Paul massif; their strontium isotopic chemistry does not preclude a genetical relation to oceanic basalts; at least one rock type from the massif could possibly be a parent material for basalt, as suggested by Melson *et al.* (1967*b*) and as indicated in table 3 and figure 6.

#### GABBROS AND BASALTS

Among the gabbros recovered from the equatorial M.A.R. we find considerable variability in mineralogy and chemistry. Thus, in addition to ‘normal’ gabbros, characterized by the assemblages calcic plagioclase–diopside, we found iron-rich gabbros, olivine gabbros (troctolites), quartz-gabbros, and gabbros with alkaline affinities, such as nepheline gabbro (theralite). In table 5 we present the results of chemical analyses of some of these rocks. Miyashiro *et al.* (1969) indicated that gabbros from the M.A.R. show considerable differentiation taking place

along a tholeiitic trend, probably due to early crystal fractionation of calcium plagioclase and olivine during slow cooling of the melt. In the alkali-iron-magnesium diagram of figure 8 we have added to the gabbros analysed by Miyashiro *et al.* those of table 5 and one sample analysed by Melson & Thompson (1970). A 'tholeiitic' differentiation trend, parallel to the  $\text{FeO}^*$ -MgO side, is clearly visible (Miyashiro, Shido & Ewing 1970*a*). The norite P 6707-5, dredged from the Chain F.Z., is highly enriched in iron and titanium and probably represents an advanced term along such differentiation trend. A gabbro with cumulate texture described by Melson & Thompson (1970) fits along this trend. Such extensive crystal-liquid fractionation as shown by figure 8 may result in some layering of the type suggested by Melson & Thompson (1970) for the Romanche area; however, we stress that the ultramafics dredged by us from the equatorial M.A.R. are genetically independent from the gabbros, and appear not to be part of a layered complex, due to reasons stated in a previous section.

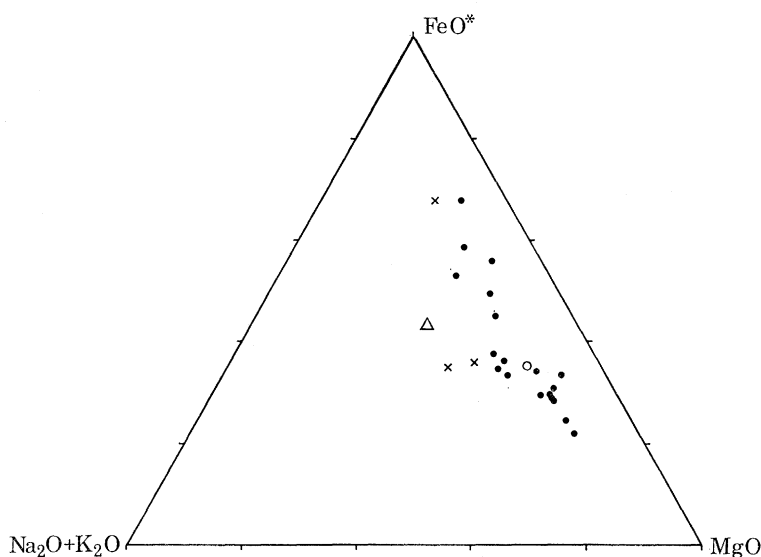


FIGURE 8. Alkali-iron-magnesium diagram for gabbros from the M.A.R. In addition to a 'tholeiitic' differentiation trend, parallel to the  $\text{FeO}^*$ -MgO side, an 'alkali' trend is visible. ●, Miyashiro *et al.* (1970); ○, Melson & Thompson (1970); Δ, nepheline gabbro; ×, other gabbros (see table 5).

In addition to the 'tholeiitic' trend, an 'alkali' trend is noticeable among the gabbros (figure 8). represented by a theralite (P 6707-25F) and an alkali gabbro (P 6707-25D). Alkali basalt magma can be produced by partial melting of mantle material at pressures (depths) larger than those required to produce tholeiitic melts (Green & Ringwood 1967). It can be assumed that during ascent and slow cooling within intrusive bodies the alkali magma will undergo differentiation independently of the tholeiitic magma. More sampling might reveal additional terms of such 'alkali' differentiation trend, which is only hinted in the diagram of figure 8. An alkali-iron-magnesium diagram for various M.A.R. basalts, including the two of table 5 (figure 9), indicates also both a 'tholeiitic' and an 'alkali' differentiation trend. As pointed out by Miyashiro, Shido & Ewing (1970*b*), the spread of the points in the direction parallel to the  $\text{FeO}^*$ -MgO side is much smaller in the basalts than in the gabbros, probably because rapid extrusion of the basalts limited the extent of the crystal-liquid fractionation processes.

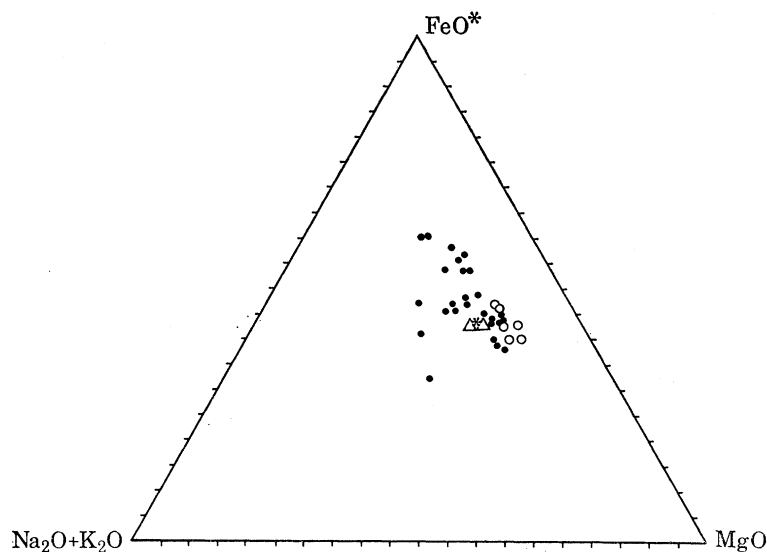
## ULTRAMAFIC ROCKS

397

TABLE 5. CHEMICAL ANALYSES OF SOME GABBROS AND BASALTS FROM THE EQUATORIAL MID-ATLANTIC RIDGE

CIPW norms are also shown.

	norite P6707-5M	gabbro P6707-25D	neph. gabbro P6707-25F	gabbro P6707-35A	basalt P6707-10	basalt P6707-25B
SiO <sub>2</sub>	43.38	51.18	46.32	50.72	48.18	46.75
Al <sub>2</sub> O <sub>3</sub>	11.89	15.26	16.84	16.61	16.25	17.19
Fe <sub>2</sub> O <sub>3</sub>	9.09	1.47	5.79	2.50	5.51	4.40
FeO	10.02	5.27	3.93	4.60	3.73	5.04
MnO	0.28	0.14	0.14	0.28	0.14	0.13
MgO	5.41	7.25	6.48	8.46	7.13	7.78
CaO	9.97	9.74	7.68	7.60	12.01	8.55
Na <sub>2</sub> O	3.00	4.09	4.36	4.03	2.39	3.20
K <sub>2</sub> O	0.14	0.74	1.01	0.08	0.25	0.70
TiO <sub>2</sub>	4.00	0.83	1.35	0.43	1.27	1.38
P <sub>2</sub> O <sub>5</sub>	1.25	0.05	0.21	0.05	0.15	0.29
H <sub>2</sub> O <sup>-</sup>	0.27	0.32	1.30	1.19	0.90	0.94
H <sub>2</sub> O <sup>+</sup>	1.25	3.79	4.50	3.21	1.88	3.35
Total	99.95	100.13	99.92	99.76	99.79	99.70
Q	2.23	—	—	—	2.75	—
Or	0.83	4.37	5.97	0.47	1.48	4.14
Ab	25.37	33.89	31.98	34.08	20.21	27.06
An	18.57	21.10	23.40	27.00	32.88	30.48
Ne	—	0.38	2.65	—	—	—
Di	18.23	21.65	10.40	8.28	20.07	7.95
Hy	9.53	—	—	15.05	8.88	8.50
Ol	—	10.81	8.26	5.92	—	7.61
Mt	13.18	2.13	8.39	3.62	7.99	6.38
Il	7.60	1.58	2.56	0.82	2.41	2.62
Ap	2.90	0.12	0.49	0.12	0.35	0.67

FIGURE 9. Alkali-iron-magnesium diagram for basalts from the M.A.R. ●, 45° N (Aumento 1968, 1969); Δ, present work (table 5); \*, Melson *et al.* (1967); ○, Nicholls *et al.* (1964).

## METAMORPHIC ROCKS

Rocks belonging to a metamorphic series reaching down to 'amphibolite facies' are represented in our dredge hauls; such rocks appear to be common at intermediate levels in the fracture zones and towards the base of the walls of the central rift valley. Among the metabasalts and metagabbros rocks belonging to a typical 'zeolite facies' were not observed by us. The metamorphic series starts with samples where olivine and plagioclase have been respectively serpentinized and saussuritized; these rocks are frequently crossed by veins with prehnite, analcite, talc and antigorite. Rocks belonging to a full 'greenschist facies' (albite-epidote-chlorite-actinolite assemblage) were found; these greenschists are similar to those reported by Melson & Van Andel (1966) in the M.A.R. at 22° N. The metamorphic series extends further to the 'amphibolite facies', characterized by the assemblage calcic plagioclase-hornblende. In some cases relict structures suggest that the parent rock of some of the amphibolites is a pyroxene gabbro. It is possible that some of the amphibolites are primary, that is, they crystallized at depth directly from a basaltic magma in presence of water, according to a mechanism suggested by Yoder & Tilley (1962). A detailed report on the metamorphic rocks from the M.A.R. will be given elsewhere.

## UPPER MANTLE AND LOWER CRUST BELOW THE EQUATORIAL ATLANTIC

The alpine-type, residual peridotites which were found to outcrop abundantly at the equatorial M.A.R. were probably emplaced as solid intrusions from below; the common occurrence in the samples of cataclastic textures and of tectonic breccias (figure 5) supports this statement. The abundance of alpine-type ultramafics suggests that this material is a common constituent of the upper mantle below the equatorial Atlantic. Thus, the data presented here lead us to postulate the existence of an upper mantle zone enriched in ancient, residual, alpine-type peridotite. Below this zone a 'pyrolitic' mantle would exist, the latter being the source material for modern oceanic gabbros and basalts (figure 10). Upwelling of 'pyrolitic' mantle and consequent segregation of basaltic liquid would result in the liquid cutting through the alpine-peridotite zone and forming a gabbro-basalt layer in the oceanic crust. In the process, blocks of alpine-peridotite mantle would also move upwards and become incorporated in the crust. Blocks of deeper, pyrolitic mantle, either undepleted or residual, may also be carried upward and become exposed; the St Peter-Paul massif would be an example.

We could speculate that the ancient, residual alpine peridotite mantle of the equatorial Atlantic is left over from the differentiation of a sialic crust, possibly the predrift continental block (Gondwana) subsequently split by the opening of the Atlantic rift.

The lack of recoveries of peridotites from fracture zones associated with the East Pacific Rise has been noted before (Melson 1969) and contrasts with the common recoveries in the Atlantic and Indian Oceans. This could signify that a sialic crust never existed in the East Pacific; as a consequence the residual alpine upper mantle zone did not develop there and blocks of it could not be extruded in the crust. This speculation agrees with predrift reconstructions of continental plates whereby the East Pacific constitutes a relatively 'primitive' ocean contrary to the Indian and Atlantic Oceans (Le Pichon 1968).

The postulated zone of ancient, alpine-type peridotite in the Atlantic upper mantle will admittedly create some puzzling problems; namely, how could such a zone persist in an



oceanic area without being swept away by mantle convective motions? Several mechanisms can be envisaged to overcome this difficulty, but none of them appear to us simple enough to be aesthetically pleasing, so we prefer at the moment to leave the question unanswered.

Miyashiro *et al.* (1970*a*) discuss two models of the oceanic crust, one whereby ultramafics are limited only to transversal fracture zones, and layer 3 is mainly gabbro–amphibolite; the other where ultramafics are ubiquitous in the oceanic crust, and are the main component of layer 3. Our dredgings indicate that ultramafics are present also in portions of the M.A.R. which are not intersected by transversal fracture zones; as a result we favour the hypothesis that ultramafics are ubiquitous in the lower crust below the Atlantic. If the M.A.R. complex is essentially created by basaltic liquids upwelling and intruding into an older peridotitic layer, the lower crust (layer 3) should be constituted both of blocks of ultramafics and of gabbro–amphibolite. This picture is supported by the finding of ultramafics above gabbro–amphibolite in some M.A.R. sections (see figure 4).

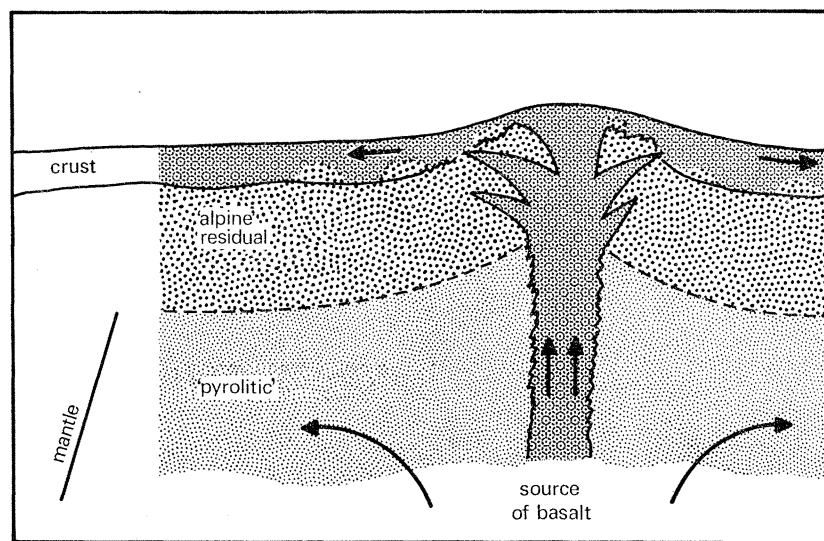


FIGURE 10. Schematic and qualitative model of the crust and upper mantle in the equatorial Atlantic, showing a zone of upper mantle enriched in residual, alpine-type peridotite, which is intruded by rising basaltic material below the axis of the ridge; as a result a peridotite–gabbro–basalt complex is formed. Source of basalt is within deeper, 'pyrolitic' mantle. Blocks of 'pyrolitic' mantle may occasionally also become incorporated in the oceanic crust. The alpine peridotite zone should exist in the Atlantic and Indian oceans, but not in the East Pacific.

#### SIMILARITIES BETWEEN THE MID-ATLANTIC RIDGE COMPLEX AND ALPINE COMPLEXES

The rock assemblage found at the equatorial M.A.R. offers strong similarities to alpine-type assemblages, as illustrated by table 6 where the petrology of four classical alpine complexes is schematically compared with that of the M.A.R. complex.

In addition to general lithological resemblances, more specific similarities can be pointed out. For instance, as stated earlier, the strontium isotopic chemistry of the M.A.R. peridotites is identical to that of alpine-type ultramafics but different from that of ultramafics from layered complexes or of peridotitic nodules in basalts.

Recent field studies of alpine complexes from various parts of the world (Reinhardt 1969; Bortolotti, Dalpiaz & Passerini 1969; Peyve 1969) indicate that the lower, peridotitic blocks are

unrelated genetically to the gabbro–basalt layer above; the peridotites have been shown generally to be much older than the gabbro–basalt and to have been intruded subsequently to their emplacement by basaltic material which gave rise to the upper gabbro–basalt blocks. These field data give independent confirmation to the interpretation of the Sr-isotopic results obtained by Stueber & Murthy (1966) for alpine peridotites, which were discussed in a previous section of this paper. The aforementioned field evidence suggests a mechanism of formation of alpine complexes very similar to that proposed by us to explain the M.A.R. complex.

TABLE 6. SCHEMATIC AND SIMPLIFIED COMPARISON OF THE M.A.R. ROCK ASSEMBLAGES WITH ASSEMBLAGES FROM SOME CLASSICAL ALPINE-TYPE COMPLEXES IN VARIOUS PARTS OF THE WORLD

equatorial Mid-Atlantic Ridge	northern Greece, Brunn (1959)	Oman, Persian Gulf; Reinhardt (1969)	Platta Nappe, Swiss Alps; Dietrich (1969)	Troodos, Cyprus; Gass (1968)
basalts, dolerites	pillow basalts, dolerites	spilitic pillow basalts, dolerites, diabases	spilitic basalts, dolerites, diabases	pillow basalts, dykes basalts
quartz diorites, nepheline gabbros, gabbros, greenschists, amphibolites	quartz-albite, pegmatites, quartz diorites	—	—	trondhjemitic
	gabbros, pyroxenites	gabbros, rodingites, amphibolites	gabbros, rodingites, pyroxenites	gabbros
picrites, lherzolites, harzburgites, dunites	lherzolites, chromitites, harzburgites, dunites	harzburgites	peridotites	chromitites, harzburgites, dunites

The concept that alpine massifs on the continents are rinds of ancient oceanic crust which was carried to the edge of the continent by sea-floor spreading, incorporated in a geosyncline and subsequently uplifted has been proposed by various authors (Brunn 1959; Dietz 1963; Thayer 1969; Peyve 1969). The similarity of the M.A.R. to alpine-type complexes supports such suggestions. However, more work is required before a genetical connexion between oceanic ridges and alpine complexes can be accepted without reservations.

#### SUMMARY AND CONCLUSIONS

(1) Rocks dredged from the equatorial Mid-Atlantic Ridge indicate that extensive peridotite–gabbro and amphibolite–basalt complexes exist in that region.

(2) The ultramafics, excluding those outcropping at the St Peter–Paul massif, are not related genetically to the gabbros and basalts. They are residual and were probably depleted of lithophile elements at some early stage of their history.

(3) The gabbros show considerable crystal–liquid fractionation. Some of the gabbros have alkali affinities.

(4) A residual, alpine-type peridotite zone probably exists in the upper mantle below the equatorial Atlantic. Basaltic liquids, formed deeper in the mantle, upwell, intrude into the residual peridotite zone, and give rise to the gabbro–amphibolite–basalt complex in the crust.

(5) The lower crust in the Atlantic consists of blocks of serpentinized peridotite intermixed with gabbro–amphibolite.

(6) The M.A.R. complex offers close similarities to alpine complexes from various parts of the world.

We thank R. P. Von Herzen for the bathymetric data on the Vema Fracture. The research was supported by National Science Foundation grants GA-1602 and GA-4569 and the Office of Naval Research contract Nonr 4008-02. Contribution No. 1523 from the Institute of Marine and Atmospheric Sciences.

REFERENCES (Bonatti *et al.*)

- Aumento, F. 1968 The Mid-Atlantic Ridge near 45° N—basalts from the area of Confederation Peak. *Can. J. Earth Sci.* **5**, 1.
- Aumento, F. & Loncarevic, B. D. 1969 The Mid-Atlantic Ridge near 45° N—Bald Mountain. *Can. J. Earth Sci.* **6**, 11.
- Bonatti, E. 1968 Ultramafic rocks from the Mid-Atlantic Ridge. *Nature, Lond.* **219**, 363.
- Bonatti, E., Ferrara, G. & Honnorez, J. 1970 Equatorial Mid-Atlantic Ridge: petrological and Sr-isotopic evidence for an alpine-type rock assemblage. *Earth Planet. Sci. Lett.* (in the Press).
- Bonatti, E., Emiliani, C. & Honnorez, J. 1970 Hydrothermal carbonate breccias from the Mid-Atlantic Ridge. (In preparation.)
- Bortolotti, V., Dalpiaz, G. V. & Passerini, P. 1969 Ricerche sulle ofioliti delle catene alpine—Nuove osservazioni sul massiccio di Vourinos (Grecia). *Boll. Soc. geol. ital.* **88**, 35.
- Brunn, J. H. 1959 La dorsale medio-atlantique et les épanchements ophiolitiques. *C. r. Soc. géol. Fr.* **8**, 234.
- Brunn, J. H. 1961 Les sutures ophiolitiques. *Revue Géogr. phys. Géol. dyn.* **4**, 89.
- Cann, J. R. 1968 Geological processes at mid ocean ridge crests. *Geophys. J.* **15**, 331.
- Christensen, N. I. 1970 Composition and evolution of the oceanic crust. *Marine Geol.* **8**, 139.
- Dietrich, V. 1969 Die Ophiolithe des Oberhalbsteins und das Ophiolith material der ostschweizerischen Molasseablagerungen. Ph.D. Thesis, University of Zurich.
- Dietz, R. S. 1963 Alpine serpentinites as oceanic rind fragments. *Bull. geol. Soc. Am.* **74**, 947.
- Gass, J. G. 1968 Is the Troodos massif of Cyprus a fragment of Mesozoic ocean floor? *Nature, Lond.* **220**, 39.
- Green, D. H. & Ringwood, A. E. 1963 Mineral assemblages in a model mantle composition. *J. geophys. Res.* **68**, 937.
- Green, D. H. & Ringwood, A. E. 1967 The genesis of basaltic magma. *Contr. miner. Petrol.* **15**, 103.
- Hart, S. R. 1965 Potassium, rubidium and strontium in the ultramafic rocks of St Paul's Islands. *Geol. Soc. Am. Special Paper* **82**, 86.
- Hess, H. H. 1962 History of the ocean basins. In *Petrologic studies* (Buddington volume), p. 599. Geological Society of America.
- Hurley, P. M. 1967 Rb<sup>87</sup>–Sr<sup>87</sup> relationships in differentiation of the mantle. In *Ultramafic rocks* (ed. P. J. Wyllie), pp. 372–373. New York: Wiley & Sons.
- Le Pichon, X. 1968 Sea floor spreading and continental drift. *J. geophys. Res.* **73**, 3661.
- Melson, W. G. 1969 Preliminary results of a geophysical study of portions of the Juan de Fuca Ridge and Blanco Fracture Zone. *ESSA Technical Memorandum C-GSTM* **6**.
- Melson, W. G. & Van Andel, T. H. 1966 Metamorphics in the Mid-Atlantic Ridge, 22° N latitude. *Marine Geol.* **4**, 165.
- Melson, W. G., Jarosewich, E., Bowen, V. T. & Thompson, G. 1967a St Peter–Paul Rocks, a high temperature mantle derived intrusion. *Science, N.Y.* **155**, 1532.
- Melson, W. G., Jarosewich, E., Cifelli, R. & Thompson, G. 1967b Alkali olivine basalt dredged near St Peter–Paul Rocks. *Nature, Lond.* **215**, 381.
- Melson, W. G. & Thompson, G. 1970 Layered basic complex in oceanic crust, Romanche Fracture, Atlantic Ocean. *Science, N.Y.* **168**, 817.
- Miyashiro, A., Shido, F. & Ewing, M. 1969 Composition and origin of serpentinites from the Mid-Atlantic Ridge near 24° and 30° north latitude. *Contr. Miner. Petrol.* **23**, 117.
- Miyashiro, A., Shido, F. and Ewing, M. 1970a Crystallization and differentiation in abyssal tholeiites and gabbros from Mid-Oceanic ridges. *Earth Planet. Sci. Lett.* **7**, 361.
- Miyashiro, A., Shido, F. & Ewing, M. 1970b Petrologic models for the Mid-Atlantic Ridge. *Deep Sea Res.* **17**, 109.
- Nicholls, G. D., Nalwalk, A. J. & Hays, E. E. 1964 The nature and composition of rock samples dredged from the Mid-Atlantic Ridge between 22° N and 52° N. *Marine Geol.* **1**, 333.
- Peyve, A. V. 1969 Oceanic crust of the geologic past. *Geotectonics* **4**, 210.
- Reinhardt, B. M. 1969 On the genesis and emplacement of ophiolites in the Oman Mountains geosyncline. *Schweiz miner. petrogr. Mitt.* **49**, 1.

- Stueber, A. M. & Murthy, V. R. 1966 Strontium isotope and alkali element abundances in ultramafic rocks. *Geochim. cosmochim. Acta* **30**, 1243.
- Thayer, T. P. 1969 Peridotite-gabbro complexes as key to the petrology of mid oceanic ridges. *Bull. Geol. Soc. Am.* **80**, 1515.
- Van Andel, T. H. 1970 Structure of the Ascension Fracture Zone. *Trans. Am. Geophys. U.* **51**, 330 (abstract).
- Van Andel, T. H., Corliss, J. B. & Bowen, V. T. 1967 The intersection between the Mid-Atlantic Ridge and the Vema Fracture Zone in the North Atlantic. *J. Mar. Res.* **25**, 343.
- Yoder, H. S. & Tilley, C. E. 1962 Origin of basalt magmas. *J. Petrol.* **3**, 342.

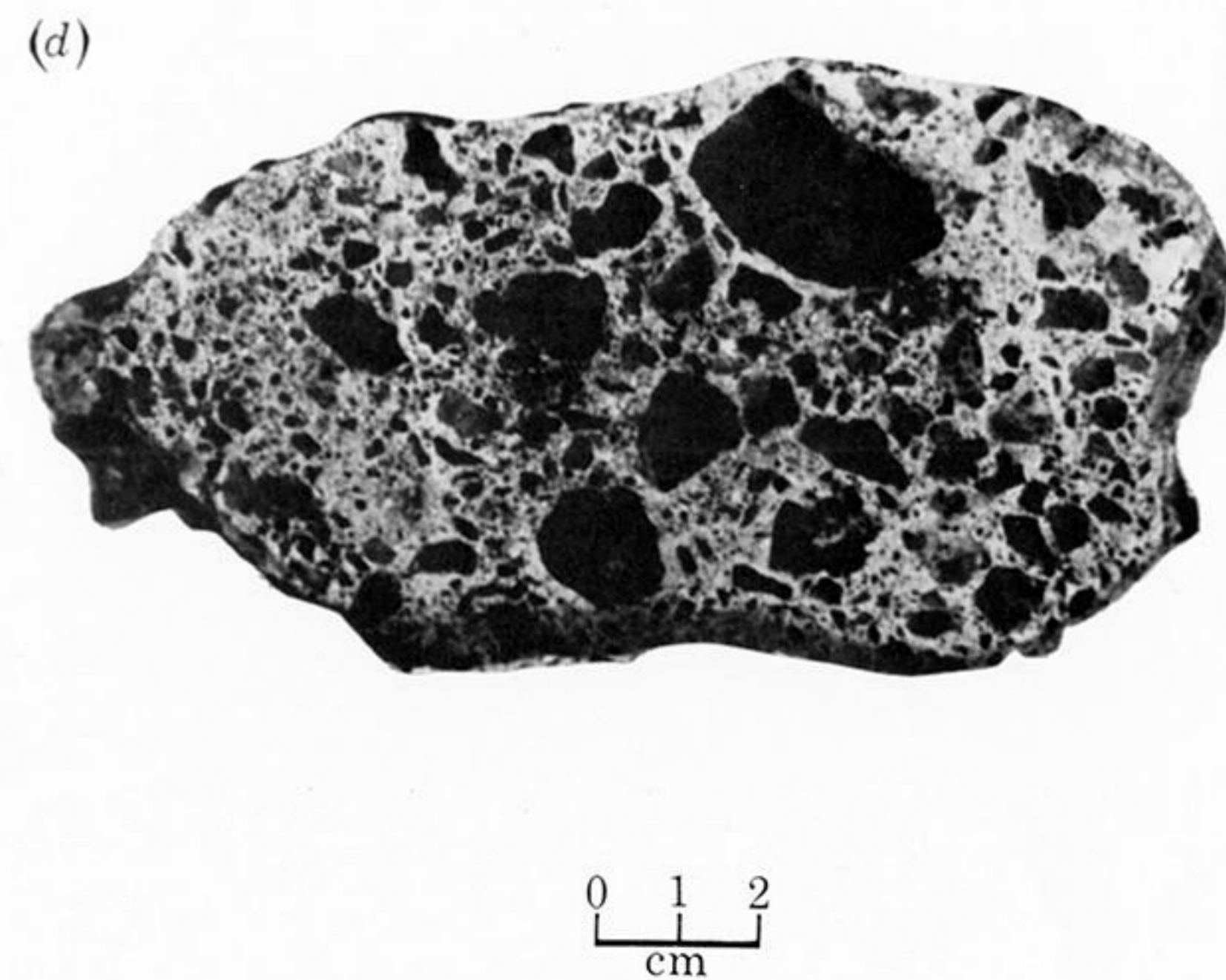
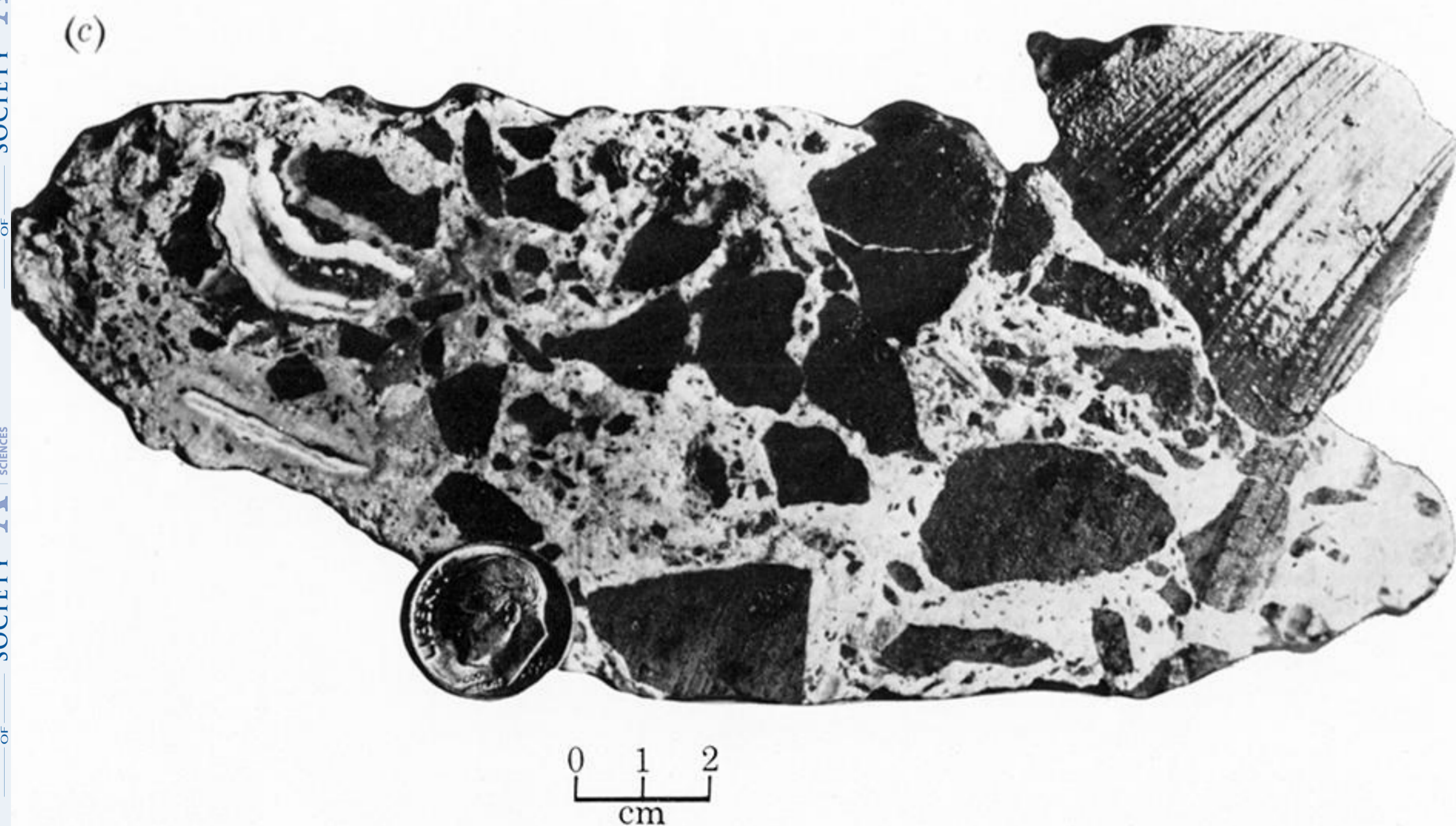
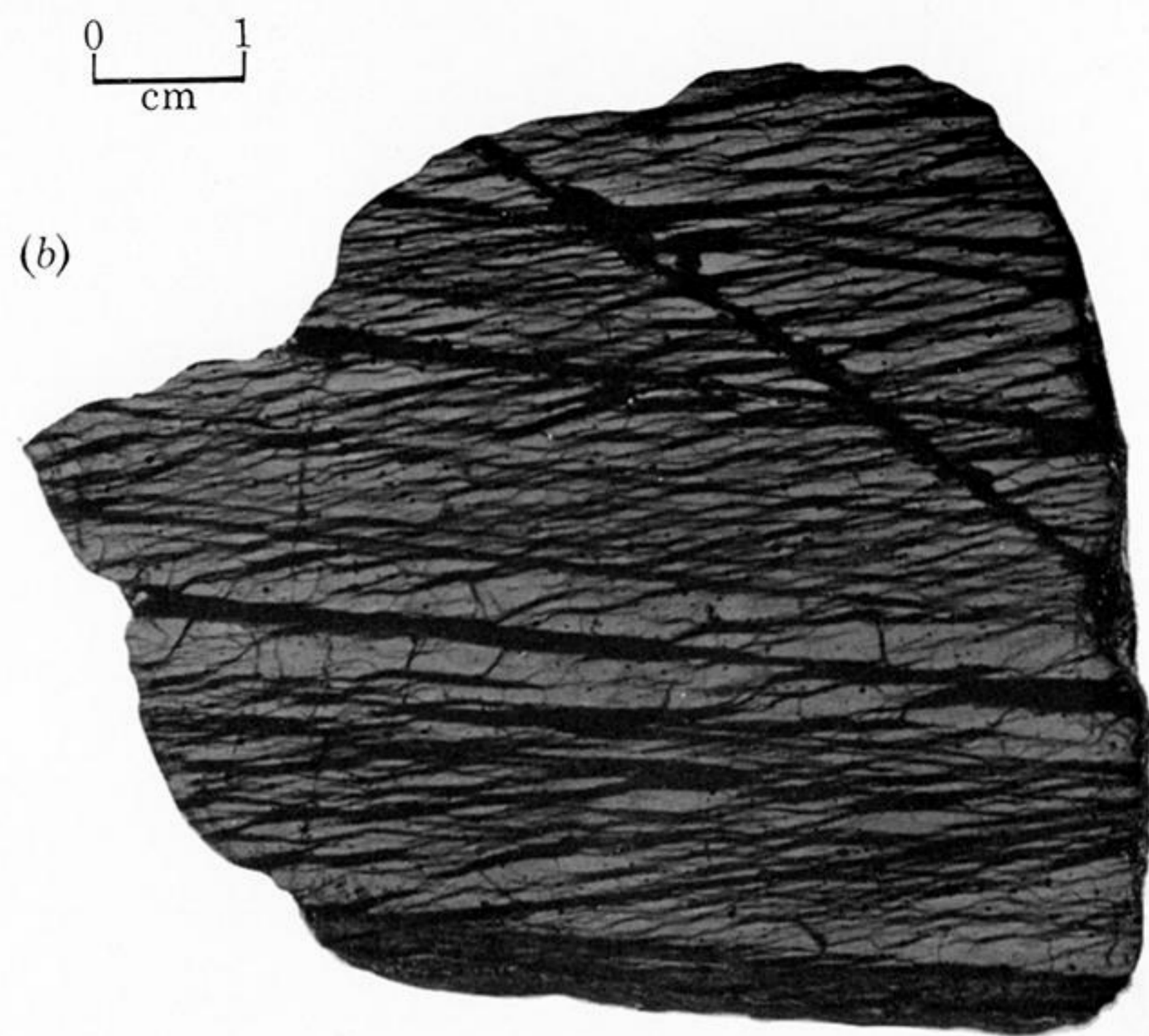
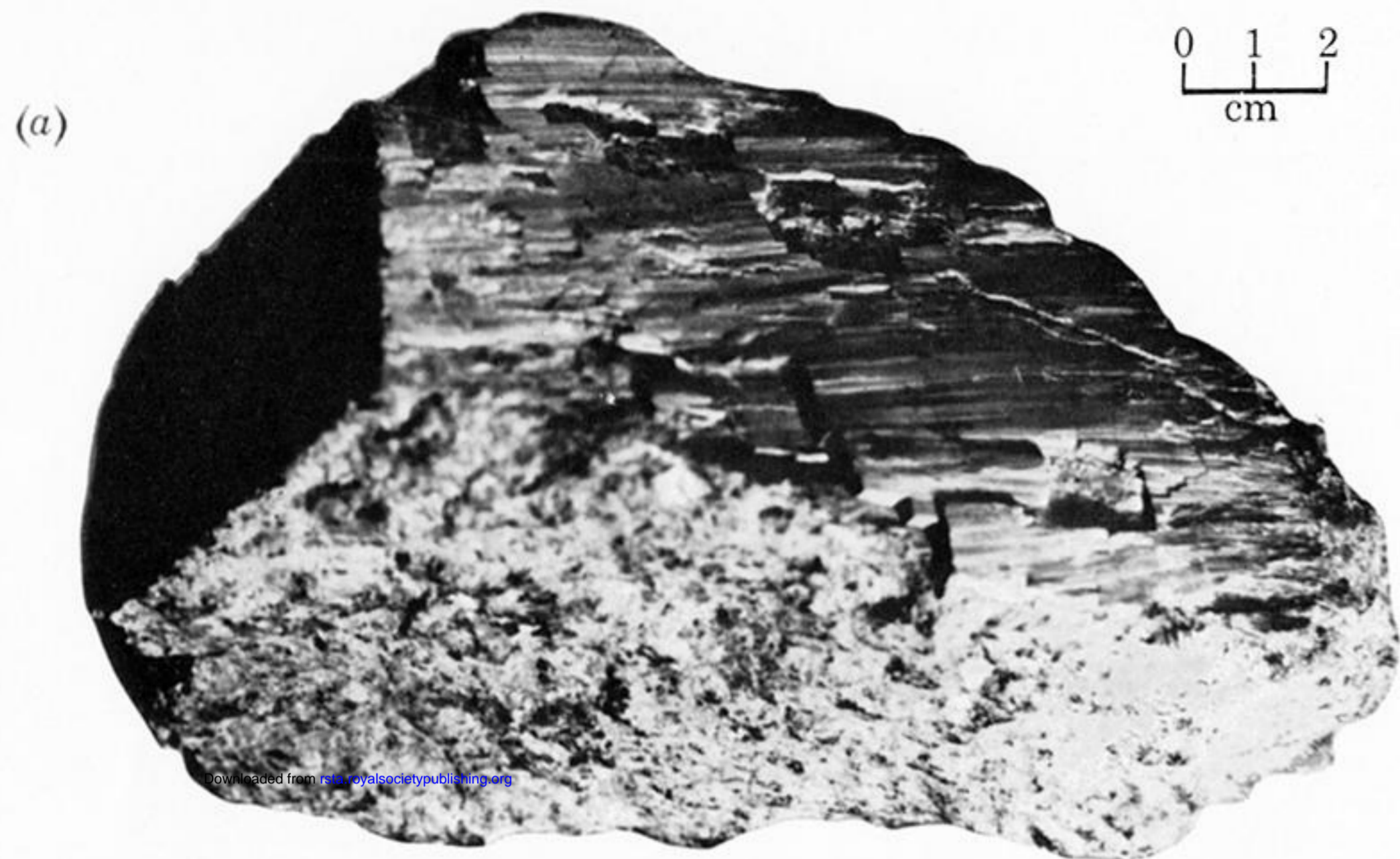


FIGURE 5. Photographs of rock specimens from the equatorial M.A.R. A, slickensided surface on peridotite from Romanche F.Z.; B, strain fabrics in serpentinite from Romanche F.Z.; C, peridotite breccia in calcite-aragonite matrix from Romanche F.Z.; D, same as C, from the Vema F.Z.